






Article

The Effect of Bone Ash on the Physio-Chemical and Mechanical Properties of Clay Ceramic Bricks

Numfor Linda Bih ^{1,*}, Assia Aboubakar Mahamat ^{1,2}, Chukwuemeka Chinweze ³, Olugbenga Ayeni ^{1,4},
Hounkpe Jechonias Bidossèssi ⁵, Peter Azikiwe Onwualu ¹ and Emmanuel E. Boakye ^{1,6}

¹ Department of Materials Science and Engineering, African University of Science and Technology, Abuja 900100, Nigeria; aassia@aust.edu.ng (A.A.M.); oayeni@aust.edu.ng (O.A.); aonwualu@aust.edu.ng (P.A.O.); kudor7@aol.com (E.E.B.)

² Department of Civil Engineering, Nile University of Nigeria, Abuja 900100, Nigeria

³ Department of Agricultural Engineering, Federal University of Technology, Owerri 460232, Nigeria; farmindustries@yahoo.com

⁴ Department of Building, Faculty of Environmental Design, Ahmadu Bello University, Zaria 810211, Nigeria

⁵ Laboratory of Geology, Mines and Environment, Faculty of Sciences and Technology, University of Abomey-Calavi, Cotonou 444, Benin; jecolune2@yahoo.fr

⁶ UES Inc., Dayton, OH 45433, USA

* Correspondence: nlinda@aust.edu.ng

Abstract: Bone ash waste can be used to fabricate clay ceramic bricks, consequently managing their pollution of the environment. This is because bone ash (BA) and clay predominantly consist of calcium and alumina-silicate, respectively, which are components of clay ceramic brick (CCB) materials. This study aims to investigate the effect of bone ash and temperature on the physio-chemical and mechanical properties of CCB. Different percentages of bone ash (5%, 10%, 15%, and 20%) were added to clay and heat treated at temperatures of 100 °C, 300 °C, 600 °C, and 900 °C, and their compressive strengths were measured. Prior to the determination of their mechanical properties, the CCB chemical and phase compositions were characterized using FTIR spectroscopy and X-ray diffraction (XRD). The CCB microstructure was evaluated with scanning electron microscopy (SEM) and the compressive strength was tested. The results suggest that the addition of bone ash (10% and 15%) improves the compressive strength and water absorption properties after heat treatment of CCB at higher temperatures.

Keywords: compressive strength; bone ash; water adsorption; clay ceramic bricks; building material; agricultural waste; kaolin clay; recycle



Citation: Bih, N.L.; Mahamat, A.A.; Chinweze, C.; Ayeni, O.; Bidossèssi, H.J.; Onwualu, P.A.; Boakye, E.E. The Effect of Bone Ash on the Physio-Chemical and Mechanical Properties of Clay Ceramic Bricks. *Buildings* **2022**, *12*, 336. <https://doi.org/10.3390/buildings12030336>

Academic Editors: Lukasz Sadowski and Giuseppina Uva

Received: 30 December 2021

Accepted: 26 January 2022

Published: 10 March 2022

Publisher's Note: MDPI stays neutral with regard to jurisdictional claims in published maps and institutional affiliations.



Copyright: © 2022 by the authors. Licensee MDPI, Basel, Switzerland. This article is an open access article distributed under the terms and conditions of the Creative Commons Attribution (CC BY) license (<https://creativecommons.org/licenses/by/4.0/>).

1. Introduction

Environmental pollution and climate change awareness has increased in recent years. The emission of CO₂ from cement production is a major concern for environmentalists [1,2], which calls for an alternate cement material for construction companies [3,4]. Pozzolanic and cementitious materials are less costly and have the needed mechanical strength to serve as construction material for building purposes. A further advantage is that CCB production releases less CO₂ into the environment compared with Portland cement [5,6], which is partly owing to bone ash being an agricultural waste material [7].

Clay ceramic bricks are potential building materials that can be strengthened by the addition of some environmental waste materials. Clay ceramic bricks (CCB) are materials formed as a result of partial replacement of clay with other mineral waste such as fly ash [8], marble sludge [9], and bone ash [10], which improves the materials' mechanical properties. Typically, the mechanical properties depend on the type of mineral addition and processing temperature [11].

An increase in agricultural activities has caused an increase in agricultural waste products, resulting in environmental pollution. Consequently, research to reduce environmental

pollution through the recycling of agricultural waste products in building construction materials is in progress. It is believed that agricultural waste used in construction material can either partially or totally replace cement to reduce CO₂ emission. Among the agricultural wastes used in construction are rice husk [12], limestone [13], eggshell [14,15], palm branch fiber [16], agro waste [17], sugarcane [18], and bamboo [19]. The reuse of agricultural waste in building construction is not new, but in this manuscript, it is used to decrease environment pollution and to improve the mechanical properties of building materials [20]. Clay bricks are one of the most used materials in the construction industry owing to cheap raw materials (clay) and ease to handle [21]. In terms of handling, it affords the formation of composites by mixing with other materials such as bone ash. Bone ash is an agricultural waste [22] with cementitious properties. It is composed mainly of phosphate, calcium, and hydroxyl ions [23].

Bones from animals disposed in a landfill cause environmental pollution. Hence, the application of bone ash waste for construction material as a total replacement of cement is considered an alternative eco-friendly building material. Although bone ash is reported to have been used as a construction material, few studies have been reported on its total replacement of cement for low and high temperature clay ceramic brick (CCB) manufacturing applications. Kaolinite clay (KC) consist of alumina (10% to 25%) and silicate (40% to 60%), which are pozzolanic precursor materials for building bricks [11,24]. Dispersed SiO₂ mineral in the clay composition provides plasticity, as such affording easy molding with improved durability of clay ceramic bricks [25]. Al₂O₃ in clay contributes to an increase in compressive strength, especially if the mullite phase forms after firing [26] at temperatures above 1000 °C. Other compounds of interests in clay are CaO, Fe₂O₃, and K₂O, which also contribute to increased strength or crack formation in bricks, depending on the percentage in clay [18,27]. A constituent of more than 10% of Fe₂O₃ and CaO can cause effloresce during a longer mixing time of clay composite [28]. The chemical constituents in the brick are relevant in determining the strength of a brick. Bone ash incorporation as a total replacement of cement can compensate for micro-cracks and increase the compressive strength.

Clay bricks can be produced as traditional sun dried bricks, at a lower firing temperature [29], or a high temperature [30,31]. Obianyo et al. (2020) mixed bone ash, hydrated lime, and laterite soil dried in oven, sun, and room temperature environments for bricks. They found a low compressive strength less than 5 MPa from bone ash stabilized soil [32] as a result of low temperature drying. Bhuiya et al. (2021) studied the effect of the bone ash on geopolymer composite for 24 h at 50 °C. They measured a compressive strength of 38.3 MPa and 36.6 MPa upon addition of 10% and 5% bone ash, respectively. Metakaolin and chemical additive such as potassium hydroxide were used to obtain the high compressive strength of 38.3 MPa [33].

This study aims to improve the compressive strength and durability of clay ceramic bricks by using bone ash as a total replacement for cement at both low and high temperatures without the use of any chemical additive.

2. Materials and Methods

2.1. Materials and Sample Preparation

Kaolin clay (KC) was bought from Ushafa Social Development Secretariat FCT Abuja Nigeria. The clay was soaked in water for a month to improve the clay properties such as plasticity and washed to remove impurities. The washed kaolin clay was allowed to settle down for one week, decanted, and dried at room temperature. The kaolin clay (KC) was oven-dried at 110 °C for 72 h, milled, and the fine particles were sieved with a 150 µm size sieve. Bone ash (BA) was sourced from Oweri Nigeria, milled, and sieved at 75 µm size. KC/BA powders of compositions 100:0, 95:5, 90:10, 85:15, and 80:20 were thoroughly mixed and compressed in a 5 cm × 5 cm × 5 cm mold. The KC/BA composites were air-dried for 21 days and fired at temperatures of 100 °C, 300 °C, 600 °C, and 900 °C. The raw materials

were characterized, and the physico-chemical and mechanical properties of clay ceramic bricks (Figure 1) were investigated.



Figure 1. Clay ceramic bricks.

2.2. Characterization of Materials

X-ray fluorescence (XRF) Thermo Scientific (ARL Quant'x model) Epsilon Spectrometer was used for the chemical composition analysis of clay and bone ash. Fourier-transform infrared (FT-IR) spectroscopy Thermo Scientific (Nicolet™ iS™5 model) was used for functional group analysis of clay, bone ash, and clay ceramic bricks (CCB). X-ray diffraction (XRD) Thermo scientific model (ARL'XTRA X-ray, Rotreuz) was used for phase analysis of the materials using the following set parameters. The XRD patterns were measured at 40 mA and 45 kV under CuK α radiation ($\lambda = 1.5406 \text{ \AA}$) from 5 to 75° 2 θ with the scan step rate of 0.03° 2 θ /min. The surface morphology and elemental composition of the clay ceramic bricks were determined with scanning electron microscope (SEM/EDX) using Carl Zeiss Model Evo LS10 after polishing and coating samples with gold to prevent sample charging.

2.3. Physio-Chemical and Mechanical Properties of Clay Ceramic Bricks' Measurement

The bulk density, water absorption, and apparent porosity of clay ceramic bricks at 600 °C and 900 °C were determined using the British Standards for clay ceramics (1985) [34]. The clay ceramic bricks (CCB) were soaked completely for 24 h in water, the samples were removed from water, and excess water was wiped from the surface of CCB. The bricks were suspended in water for a minute, removed, and re-weighed. Water absorption measurements were done for brick samples only heat-treated at 600 °C and 900 °C. The dry weight (M_s), the saturated weight of wet bricks in air (M), and the suspended weight in water (M_w) of the samples were noted. The bulk density, apparent porosity, and water absorption were calculated from Equations (1)–(3). The compressive strength of CCB was determined using the compressive testing machine model ELE ADR (series No.1912-3-00282, UK). A replicate of five samples for each clay/bone ash composition was measured (Table 1) and the average compressive strength was recorded. The samples were pre-dried at room temperature (26 °C) for 21 days before heat treatment. The weight of each brick was measured using an electronic balance and the actual size of each sample was taken using a Vernier Calipers before and after heat treatment. The clay ceramic bricks were fired at temperatures of 100 °C, 300 °C, 600 °C, and 900 °C. The compressive testing was done at a 0.250 MPa/s loading rate under monotonic failure. Compressive strength (CS) was calculated from the failure load (F) divided by surface area (A) of the bricks (Equation (4)).

$$\text{Bulk density} = \frac{M_s}{M_s - M_w} \quad (1)$$

$$\text{Apparent porosity (\%)} = \frac{M - M_s}{M - M_w} \times 100 \quad (2)$$

$$\text{Water absorption (\%)} = \frac{M - M_s}{M_s} \times 100 \quad (3)$$

$$\text{CS (MPa)} = \frac{F(N)}{A(\text{mm}^2)} \quad (4)$$

Table 1. Sample composition and heat treatment temperature.

Sample Name	Bone Ash (%)	Clay (%)	Temperature (°C)
100C	-	100	100, 300, 600, and 900
5BAC	5	95	100, 300, 600, and 900
10BAC	10	90	100, 300, 600, and 900
15BAC	15	85	100, 300, 600, and 900
20BAC	20	80	100, 300, 600, and 900

3. Results and Discussion

3.1. Chemical Characterization of Clay Ceramic Bricks

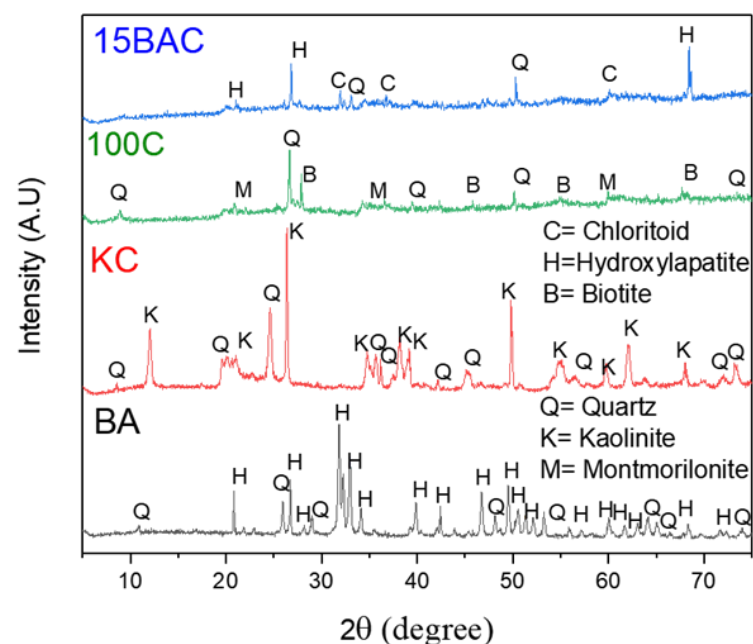
3.1.1. XRF Characterization of Raw Materials

The chemical composition of bone ash (BA) and kaolin clay (KC) is presented, as shown in Table 2. The result showed that P_2O_5 (34.50%) and CaO (42.87%) were the major chemical constituents in BA. This suggests that the major inorganic component of bone ash may be hydroxyapatite ($Ca_5(PO_4)_3OH$). The major components of KC are alumina (54.81%) and silica (22.72%); Table 2. This result was consistent with the chemical composition of BA and KC from the obtained SEM-EDX analysis shown in Figure 2. The combined constituent of ferric oxide (Fe_2O_3), potassium oxide (K_2O), titanium oxide (TiO_2), manganese oxide (MgO), calcium oxide (CaO), and titanium oxide (TiO_2) was more than 10%, suggesting the clay to be a low refractive material [9].

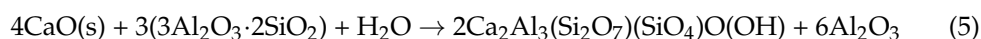
Table 2. XRF analysis of raw materials.

Chemical Composition	Oxide Percentage of BA (%)	Oxide Percentage of KC (%)
P_2O_5	34.50	-
CaO	42.87	0.73
Fe_2O_3	-	9.23
SiO_2	11.54	54.81
Al_2O_3	1.84	22.72
MgO	-	3.22
TiO_2	0.05	1.74
K_2O	0.09	2.77
LOI*		1.7

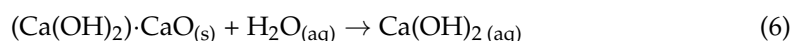
* LOI: loss on ignition (at 1000 °C).

**Figure 2.** XRD patterns of clay ceramic bricks (100C and 15BAC), KC, and BA.

The rich alumina-silicate chemical composition in clay indicated that the material is kaolinite clay, and this was further confirmed by the XRD analysis (Figure 2). The chemical composition of a material contributes to the compressive strength. The increased in compressive strength was a result of cementitious properties owing to the pozzolanic reactions between the calcium oxide in bone ash, alumino-silicate in the clay, and water (Equation (5)) [35].



The reaction between calcium oxide and water has cementitious properties, which enables the clay ceramic bricks' strength to increase (Equation (6)).



The Ca(OH)_2 formed during cementitious reactions from the chemical components of BA and water is also suggested to improve compressive strength. Calcium hydroxide [Ca(OH)_2], also known as portlandite, is then further reacted with silicate from the alumina-silicate clay to give a calcium silicate hydrate ($\text{CaSiO}_3 \cdot 2\text{H}_2\text{O}$) [36] as a cementitious compound, leading to the increase in the compressive strength of the ceramic clay bricks (Equation (7)).



3.1.2. XRD Analysis

Figure 2 shows diffraction patterns of bone ash (BA), kaolin clay (KC), and clay ceramic bricks (CCB). The XRD patterns showed that the two major phases are kaolinite and quartz in KC. Hydroxyapatite is the major crystalline phase in bone ash (BA) and has some traces of quartz that are also present in sample 15BAC [37,38]. The control sample 100C (0% bone ash) showed that the three phases of XRD patterns are quartz, biotite, and montmorillonite. The ceramic clay bricks (15BAC) present three XRD patterns of hydroxyapatite, chloritoid, and quartz. The XRF (Table 2) also suggested hydroxyapatite in bone ash, as well as Mg, Fe, and K in kaolin clay, which is consistent with the XRD results [35].

3.1.3. FTIR Analysis

The FTIR spectra were conducted in the range $400\text{--}4000\text{ cm}^{-1}$. The observed bands for bone ash, clay, and clay ceramic bricks (CCB) are presented in Figure 3. The characteristic spectra bands around 3556 cm^{-1} correspond to the hydroxyl (H-O-H, O-H) stretching bonds of hydroxyapatite in bone ash. The H-O-H stretching group showed two peaks close to each other at 3620 cm^{-1} and 3695 cm^{-1} in the clay spectra that shift to 3472 cm^{-1} broad bands in the CCB spectra. The vibrational bands at 2022 cm^{-1} are due to the presence of the CO_2 group in the bone ash. A similar vibration band at 2361 cm^{-1} , corresponding to clay, appeared at the same intensity as the CO_2 group [39]. The 1650 cm^{-1} and 1636 cm^{-1} bands are associated with amide (NH_2) stretching groups on bone ash and CCB, respectively. The band at 1412 cm^{-1} assigned to bone ash spectra is due to CO_3^{-2} vibrations. The bone ash PO_4^{-2} stretching vibrational bands were observed at 1094 cm^{-1} , 1058 cm^{-1} , 630 cm^{-1} , and 561 cm^{-1} , and is in agreement with the XRF (Table 2) results. Further, the results of this study are consistent with the work of Chakraborty et al. (2015) and Rana et al. (2017) [40,41]. The clay spectra band at 1114 cm^{-1} and 1032 cm^{-1} showed the presence of a strong asymmetrical Si-O stretching vibration bond that confirmed the presence of kaolinite and quartz in the XRD of clay (Figure 1). The band at 912 cm^{-1} corresponds to Al-O stretching bonds in kaolin clay. The bands at 537 cm^{-1} and 428 cm^{-1} are attributed to O-H bending bonds of clay. The band at 460 cm^{-1} is assigned to Al-O-Si vibration bonds on the CCB spectra [42].

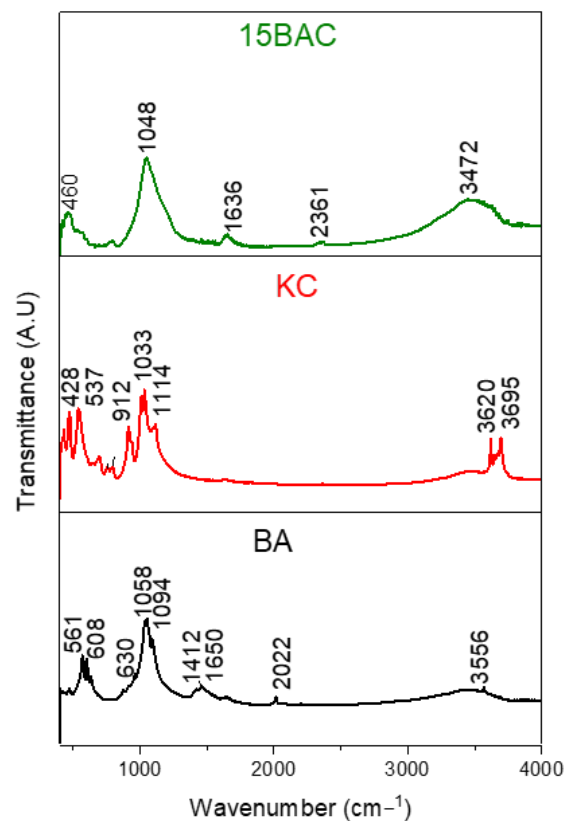


Figure 3. FTIR spectra of clay ceramic bricks (15BAC), KC, and BA.

3.1.4. SEM Micrograph Analysis

Figures 4 and 5 represent SEM micrographs of raw materials (bone ash and clay) and clay ceramic bricks at different temperatures, respectively. The light colored particles of bone ash are due to the presence of CaO [43]. The bone ash SEM showed irregularly shaped hydroxyapatite particles with different sizes. Further, EDX showed the presence of Al and Si (Figure 6).

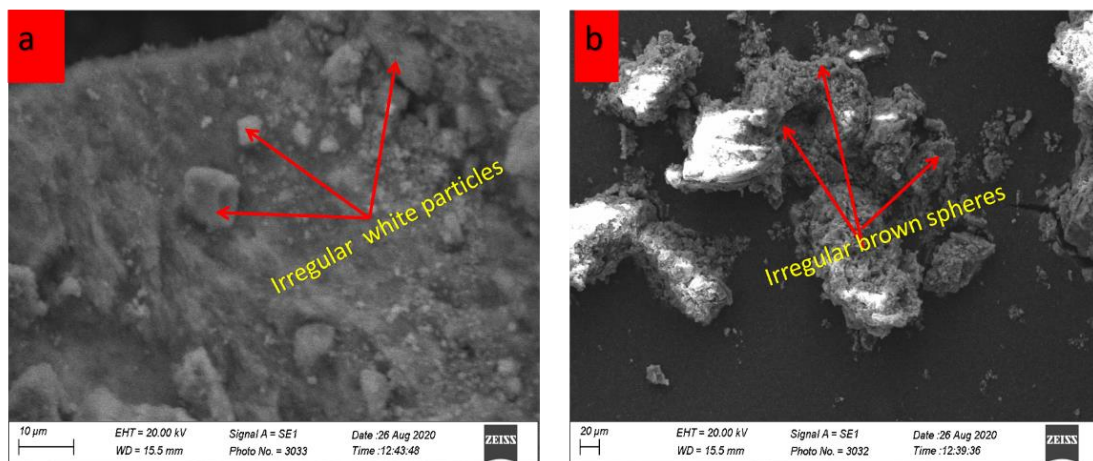


Figure 4. SEM micrograph of (a) bone ash and (b) clay.

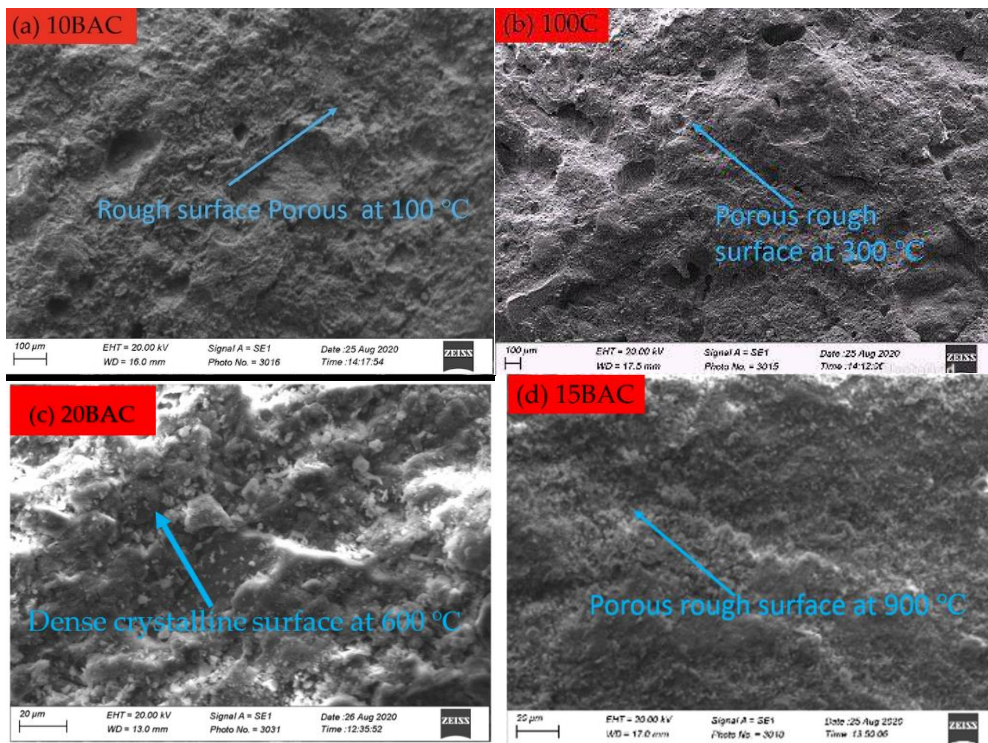


Figure 5. SEM micrograph of clay ceramic bricks at (a) 100 °C, (b) 300 °C, (c) 600 °C, and (d) 900 °C.

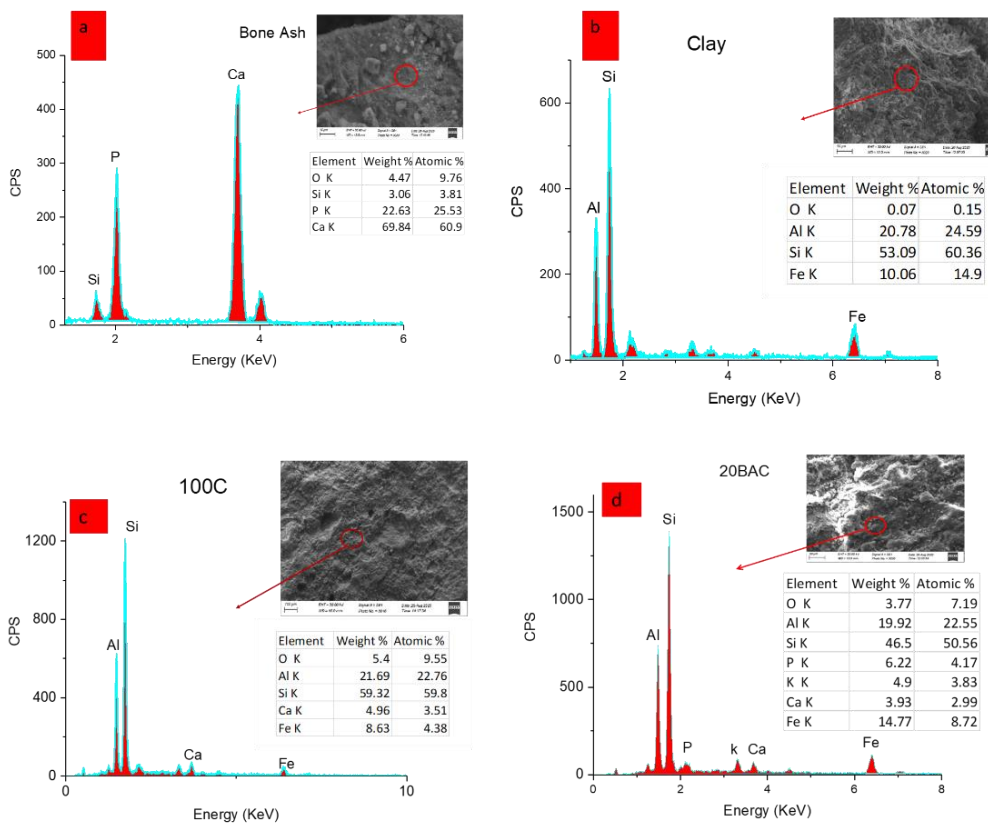


Figure 6. EDX analysis of (a) bone ash, (b) clay, (c) control sample (100C), and (d) clay ceramic brick with 20% bone ash.

Figure 5 illustrates SEM micrographs of brick materials that have been heat-treated at 100 °C, 300 °C, 600 °C, and 900 °C. It can be seen from this figure that the ceramic bricks became denser as temperature increased from 100 °C to 900 °C; Figure 5. The irregular crystalline particles of bone ash bonded and fused eventually with the irregular sphere particles of clay, decreasing the apparent porosity as the temperature increased. Generally, bone ash addition increased the quantity of hydroxyapatite and, therefore, increased the cementitious reaction as the temperature became higher [35]. The surface of the ceramic brick produced at 100 °C became smoother owing to an improved cementation reaction within the clay ceramic brick (Figure 5) [35]. Dense crystalline phases on CCB at 600 °C and 900 °C were due to sintering clay bone ash composite, as observed by Johari et al. (2010) [27]. Increasing the temperature forms denser CCB.

Similar to the work of Ifka et al. (2012) [44], the EDX analysis showed calcium and phosphorus as the major constituents in bone ash, with some traces of Si (Figure 6a). EDX also showed Si and Al as the major constituents in clay with a trace of Fe. The minor constituent elements present, including Fe, Mg, and K, were more than 10% (Table 2). No surface cracks were observed on CCB for bricks fired up to 900 °C. Obianoyo et al. (2020) have shown that hydroxyapatite in bone ash and Si in laterite soil improve the cementitious property and compressive strength of bricks. In our results, the presence of hydroxyapatite, as evidenced by X-ray and EDX with Ca and Si, helped improve the cementitious property of the CCB and resulted in higher compressive strengths.

3.2. Physical Characterization of Raw Materials and Clay Ceramic Bricks

3.2.1. Plasticity Analysis of Bricks

Brick samples dried at room temperature for 21 days had no observable defects, such as bloating or cracks. After fracturing samples heat-treated to 900 °C, there was no observed dark coloration on the fracture surface, suggesting that any organic residues were completely burned out after the 900 °C heat treatment. The physical properties of raw materials analyzed before the production of the clay ceramic bricks indicated that bricks fired above 1200 °C will crack and effloresce owing to the over 10% minor chemical constituents in clay (Table 2). The Atterberg Limits according to BS1377 standard [45] were used to characterize the physical properties of clay. An amount of 400 g of clay was mixed with distilled water for 10 min in a glass plate. Using a Palette knife, the paste was transferred in a brass cup while tapping gently to avoid air trap, and excess clay was removed. The penetration cone was placed at the surface of paste and the dial gauge was lowered to touch the cone shaft, and the first reading was recorded. The cone was released for a period of 5 s and the dial gauge was released to touch the cone shaft. The second reading was taken and the difference between readings was recorded during penetration. The process was repeated until the overall range was not more than 1 mm. The process was repeated five times. A graph of moisture content versus penetration of cone was plotted and the moisture content corresponding to 20 mm is the liquid limit. The clay sample retained material on a 425 µm sieve was removed and 40 g of sieved clay mixed with distilled water was placed in a glass plate. The paste was allowed to dry partially and became plastic to roll. The clay was rolled into a ball with fingers until slight cracks due to drying were noticed. The rolled clay was divided into two halves of 20 g each and each half was further divided into four parts. The different parts were rolled into threads until reaching a 3 mm diameter and the first crumbling point was taken as the plastic limit. The plastic limit, liquid limit, and moisture content are important parameters in forming clay bricks (Table 3). The plasticity of clay is given by its plasticity index. The plasticity index of clay was measured by calculating the difference between the liquid limit and plastic limit. The plasticity index for kaolin clay is usually between 30% and 35% [46]. A reddish brown coloration of clay observed as spherical particles (Figure 4b) is due to the presence of iron oxides [47]. The presence of iron oxide in clay gives clay a low plasticity. The presence of Fe in the clay was confirmed by the EDX analysis (Figure 6). Therefore, the reddish brown clay used in this work had a low plasticity index of ~15.32%. Consequently, the plasticity of

the clay material was improved by soaking in water for a month prior to being used. The clay liquid limit of 41.8% was good enough for handling and molding.

Table 3. The physical properties of KC (test method BS1377).

Physical Properties	Percentage
Liquid limit	41.8
Plastic limit	26.48
Average moisture content	42.51
Average linear shrinkage	7.79
Plasticity index	15.32
Sieve size	425 μm
Colour	Reddish brown

3.2.2. Bulk Density

The bulk densities of clay ceramic bricks are presented in Figure 7. Clay ceramic bricks samples at 100 °C and 300 °C were not verified for bulk density, apparent density, and apparent porosity owing to the high water absorption of the bricks and the samples' dissolution in water. The bulk density of clay ceramic bricks (CCB) was between 1.59 g/cm³ and 1.81 g/cm³. Generally, the bulk density increased with the percentage of bone ash added. This could result from the increase in the reactive silica from 5BAC to 20BAC reacted with CaO, hence forming C-S-H, which caused an increase in the bulk density. The materials became denser and the pores reduced as the molecules take the place of the interstice, hence increasing the packing factor, which results in a dense material. The sample 5BAC showed a moderate bulk density of 1.59 g/cm³ and 1.62 g/cm³ at 600 °C and 900 °C, respectively. It is also suggested that the presence of a fluxing agent (K₂O, MgO, Fe₂O₃, and CaO) >10% forms liquid phase molten materials during firing at 900 °C compared with CCB fired at 600 °C, which led to increased bulk density [48]. Thus, we assume that the required minimum of hydroxyapatite in bone ash to improve the cementitious property with a moderate bulk density is ~5% and the maximum is 15%.

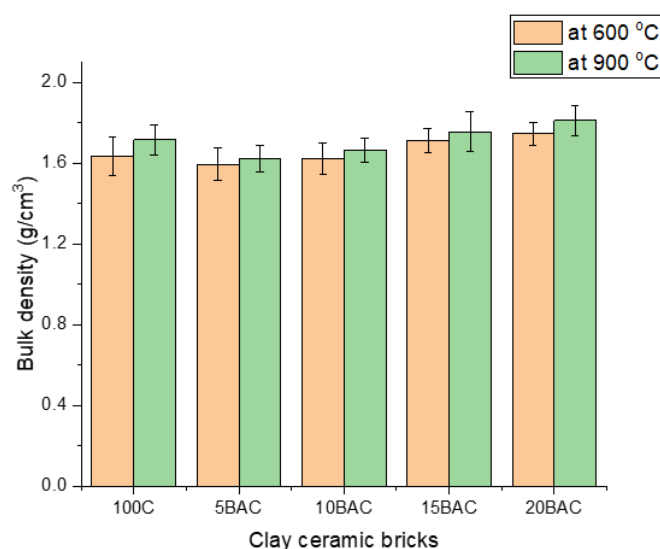


Figure 7. Bulk density of clay ceramic bricks at 600 °C and 900 °C.

3.2.3. Apparent Porosity

The apparent porosity of a clay ceramic brick is a very important parameter in building materials. Figure 8 presents the apparent porosity of clay ceramic bricks (CCB) at temperatures of 600 °C and 900 °C [34]. Apparent porosity increased from 600 °C to 900 °C and decreased from sample 100C to 20BAC. The evolution and coalescence of pores at a higher temperature might be attributed to the increase in apparent porosity at 900 °C. However,

the decrease in apparent porosity from sample 100C to 20BAC is due to the decrease in the evolution of pores as the interstice is occupied, the packing fraction of bricks increases, and thus the porosity reduces. The 100C, 5BAC, and 10BAC samples heat-treated at 900 °C had porosities of 35%, 33%, and 31%, respectively, which was congenial to clay bricks [49]. The slight increase in apparent porosity from samples 15BAC to 20BAC might be a result of the increase in pozzolanic and cementitious reaction in 20BAC at 600 °C. The apparent porosity increased with the increase in heat treatment temperature from 600 °C to 900 °C. This might have been a result of the loss of organic compounds at higher heat-treated samples at 900 °C in the brick material that caused extra pores, leading to a higher porosity.

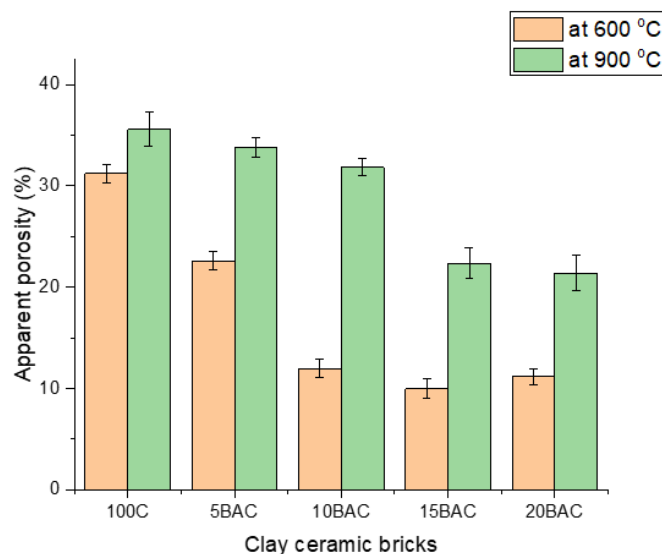


Figure 8. Apparent porosity of clay ceramic bricks at 600 °C and 900 °C.

3.2.4. Water Absorption

The effect of water absorption on clay ceramic bricks (CCB) is essential to validate their durability. The water absorption of CCB is inversely proportional to its durability. The higher the water absorption, the lower the degradation and the durability of the CCB [31].

Figure 9 shows the water absorption of clay ceramic bricks versus percentage addition of bone ash (BA) in clay at 600 °C and 900 °C. Water absorption decreased with increased BA addition, which resulted in densification from 100C to 20BAC. The increase in bulk density decreased with water absorption. This may be due to the formation of a calcium silicate hydrate (C-S-H) thin layer and calcium hydroxide (portlandite) at high temperatures, which reduce water adsorption at higher temperatures [3]. Owing to incomplete dehydration of water molecules from CCB heat-treated at 100 °C and 300 °C, the bricks collapsed totally during the water absorption test. A complete dehydration of water molecules in the consolidated CCB body and the closing of interstices at 600 °C and 900 °C prevented the CCB from completely absorbing water. A temperature as low as 600 °C is recommended to achieve low water absorption and high compressive strength to fabricate low energy cost CCB. This result agrees with the study of red brick ceramics sintered at 600 °C conducted by Monteiro et al. (2003) [29].

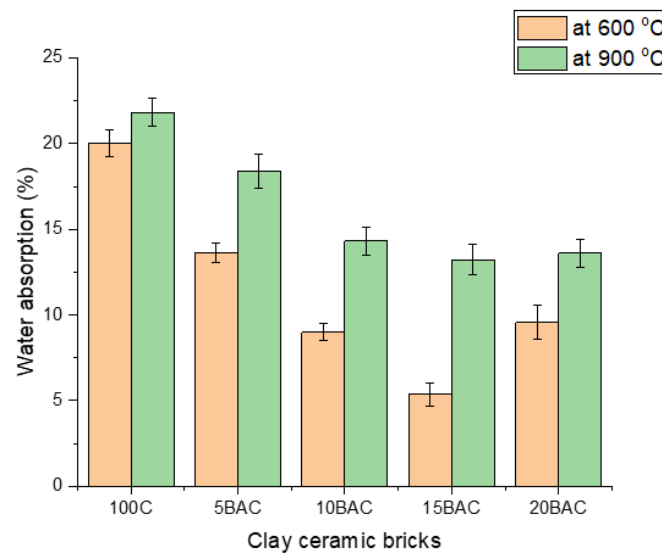


Figure 9. Water absorption of clay ceramic bricks at 600 °C and 900 °C.

3.2.5. Percent Weight Loss (%) of Clay Ceramic Bricks

The percent weight loss (Figure 10) of clay ceramic bricks (CCB) was measured by weighing the bricks after drying (W_b) in the oven and after heat treatment at temperatures of 100 °C, 300 °C, 600 °C, and 900 °C for an hour (W_a) (Equation (8)). The weight loss of CCB increased with the increasing temperature. Moreover, the weight loss increased with bone ash addition in clay. The increase in weight loss is due to the removal of water molecules and organic compounds during heat treatment at the given temperature. This correlated with the increase in apparent porosity (Figure 8) as temperature increased. CCB at 100 °C and 300 °C showed very low weight percent loss, attributed to water retention thanks to the hydrophilic nature of the samples.

$$\text{Percent weight loss (\%)} = \frac{W_a - W_b}{W_b} \times 100 \quad (8)$$

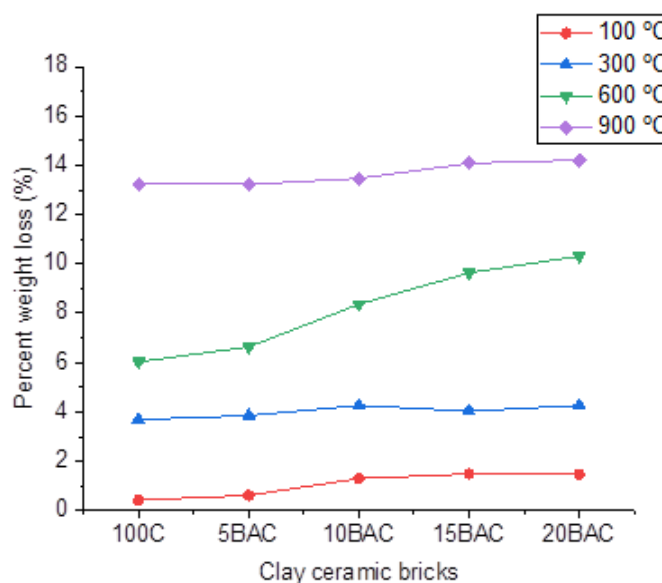


Figure 10. Percent weight loss of clay ceramic bricks after drying at 100 °C, 300 °C, 600 °C, and 900 °C.

3.3. The Effect of Bone Ash Addition and Temperature on the Compressive Strength of Clay Ceramic Bricks

The effect of bone ash addition to the compressive strength is presented in Figure 11. The bone ash addition to the clay matrix for the production of clay ceramic bricks (CCB) increased the compressive strength. Further, the compressive strength was found to increase at higher temperatures. The addition of 10% and 15% bone ash showed the highest compressive strength at all temperatures. The strength increase was highest for CCB samples processed at 600 °C and 900 °C, suggesting that the cementitious properties of bone ash are effective at higher temperatures.

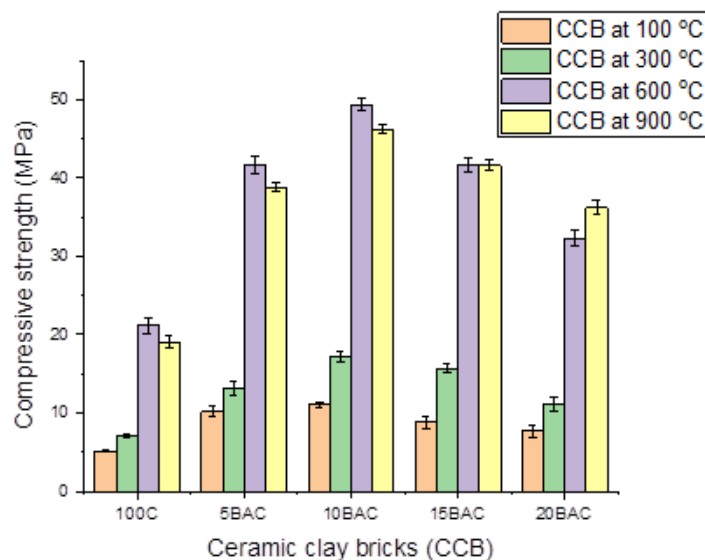


Figure 11. Compressive strength of CCB after drying at 100 °C, 300 °C, 600 °C, and 900 °C.

The addition of bone ash at different percentage levels, that is, 5%, 10%, 15%, and 20%, increased the bulk density and decreased the apparent porosity, resulting in improved compressive strength (Figures 7–9 and Figure 11). The pozzolanic and cementitious reactions that prevent pore growth lead to an increase in the bulk density, decrease in porosity, and increase in the compressive strength. Effective cementitious properties may be due to the presence of Ca and P in bone ash for CCB composite, which are absent in the control sample (100C), leading to improved compressive strength. This agrees with the XRD results indicating the presence of hydroxyapatite in 20BAC and its absence in 100C (Figure 2).

4. Conclusions

The effect of bone ash addition to a clay matrix and the effect of temperature on clay ceramic bricks (CCB) material was investigated. Bone ash addition to clay slightly improved the compressive strength for samples heat-treated at 100 °C and 300 °C, but significantly increased the compressive strength at temperatures of 600 °C and 900 °C. Therefore, the addition of bone ash helps the cementitious reaction at elevated temperatures to increase the compressive strength of CCB. The bone ash containing hydroxyapatite addition to kaolin (alumino-silicate) clay for clay composite mimics the cementitious reaction in Portland cement bricks as a construction material. Compared with bricks manufactured with clay as a control (strength of 20 MPa), bricks formed with 5%, 10%, and 15% bone ash had strengths of ~41.6 MPa, ~49.3 MPa, and 46.1 MPa, respectively. Though the compressive strengths of samples 10BAC and 15BAC showed the highest, the bulk densities were also higher than that of sample 5BAC. In addition, these samples had less water adsorption of ~20% owing to decreased porosity. At a temperature of 600 °C, the compressive strength of CCB is improved and water absorption is decreased. It is suggested that, depending on the purpose of building material, the amount of bone ash added and firing temperature should

be considered. A high temperature is required to improve the durability of the bricks to avoid high water absorption. The reduction in environment pollution, both landfill and carbon dioxide reduction, through the usage of bone ash will sustain climate change reduction, affording low-cost building materials with high compressive strengths.

Author Contributions: Conceptualization, N.L.B. and A.A.M.; methodology, C.C., O.A., and H.J.B.; software, E.E.B.; validation, E.E.B., A.A.M., and N.L.B.; formal analysis, P.A.O.; investigation, P.A.O. and O.A.; resources, H.J.B. and O.A.; data curation, N.L.B. and H.J.B.; writing—original draft preparation, A.A.M. and N.L.B.; writing—review and editing, C.C., O.A., E.E.B., and A.A.M.; visualization, N.L.B. and C.C.; supervision, E.E.B. and P.A.O.; project administration, C.C. and H.J.B.; funding acquisition, P.A.O. All authors have read and agreed to the published version of the manuscript.

Funding: This research was funded by the African Development Bank (AfDB), grant number (NMI-AIST 2100155032824) and by the Pan African Materials Institute under the World Bank African Centers of Excellence (ACE) program at the African University of Science and Technology (AUST), Abuja, Nigeria grant number (PAMI/2015/5415-NG).

Institutional Review Board Statement: Humans and animals were not involved in this study.

Informed Consent Statement: This is not applicable in this study with no human involved.

Data Availability Statement: The data presented is available on request from the corresponding author after obtaining permission of authorized person. The authors adhere to the MDPI Research Data Policies.

Acknowledgments: The authors acknowledging the support of Vitalis Anye, Abdulhakeem Bello and the laboratory technicians at AUST-Abuja.

Conflicts of Interest: The authors declare no conflict of interest.

References

- Poudyal, L.; Adhikari, K. Environmental sustainability in cement industry: An integrated approach for green and economical cement production. *Resour. Environ. Sustain.* **2021**, *4*, 100024. [\[CrossRef\]](#)
- Liu, B.; Qin, J.; Shi, J.; Jiang, J.; Wu, X.; He, Z. New perspectives on utilization of CO₂ sequestration technologies in cement-based materials. *Constr. Build. Mater.* **2021**, *272*, 121660. [\[CrossRef\]](#)
- Nwankwo, C.O.; Bamigboye, G.O.; Davies, I.E.; Michaels, T.A. High volume Portland cement replacement: A review. *Constr. Build. Mater.* **2020**, *260*, 120445. [\[CrossRef\]](#)
- Mahamat, A.; Bih, N.L.; Ayeni, O.; Onwualu, P.A.; Savastano, H.; Soboyejo, W.O. Development of Sustainable and Eco-Friendly Materials from Termite Hill Soil Stabilized with Cement for Low-Cost Housing in Chad. *Buildings* **2021**, *11*, 86. [\[CrossRef\]](#)
- Jamsawang, P.; Charoensil, S.; Namjan, T.; Jongpradist, P.; Likitlersuang, S. Mechanical and microstructural properties of dredged sediments treated with cement and fly ash for use as road materials. *Road Mater. Pavement Des.* **2020**, *22*, 2498–2522. [\[CrossRef\]](#)
- He, Z.; Shen, A.; Wu, H.; Wang, W.; Wang, L.; Yao, C.; Wu, J. Research progress on recycled clay brick waste as an alternative to cement for sustainable construction materials. *Constr. Build. Mater.* **2021**, *274*, 122113. [\[CrossRef\]](#)
- Zeidabadi, Z.A.; Bakhtiari, S.; Abbaslou, H.; Ghanizadeh, A.R. Synthesis, characterization and evaluation of biochar from agricultural waste biomass for use in building materials. *Constr. Build. Mater.* **2018**, *181*, 301–308. [\[CrossRef\]](#)
- Abbas, S.; Saleem, M.A.; Kazmi, S.M.; Munir, M.J. Production of sustainable clay bricks using waste fly ash: Mechanical and durability properties. *J. Build. Eng.* **2017**, *14*, 7–14. [\[CrossRef\]](#)
- Munir, M.J.; Abbas, S.; Nehdi, M.L.; Kazmi, S.M.S.; Khitab, A. Development of Eco-Friendly Fired Clay Bricks Incorporating Recycled Marble Powder. *J. Mater. Civ. Eng.* **2018**, *30*, 04018069. [\[CrossRef\]](#)
- Ozaki, H.; Sharma, K.; Saktaywin, W. Performance of an ultra-low-pressure reverse osmosis membrane (ULPROM) for separating heavy metal: Effects of interference parameters. *Desalination* **2002**, *144*, 287–294. [\[CrossRef\]](#)
- Khitab, A.; Riaz, M.S.; Jalil, A.; Khan, R.B.N.; Anwar, W.; Khan, R.A.; Arshad, M.T.; Kirgiz, M.S.; Tariq, Z.; Tayyab, S. Manufacturing of Clayey Bricks by Synergistic Use of Waste Brick and Ceramic Powders as Partial Replacement of Clay. *Sustainability* **2021**, *13*, 10214. [\[CrossRef\]](#)
- Moayed, H.; Aghel, B.; Abdullahi, M.M.; Nguyen, H.; Rashid, A.S.A. Applications of rice husk ash as green and sustainable biomass. *J. Clean. Prod.* **2019**, *237*, 117851. [\[CrossRef\]](#)
- Hafez, A.I.; Khedr, M.M.; Osman, R.M.; Sabry, R.; Mohammed, M.S. A comparative investigation of the unit cost for the preparation of modified sand and clay bricks from rice husk waste. *J. Build. Eng.* **2020**, *32*, 101765. [\[CrossRef\]](#)
- Minakshi, M.; Schneider, P.A.; Fichtner, M. Biowaste eggshells as efficient electrodes for energy storage. In *Valorization of Agri-Food Wastes and By-Products*; Elsevier BV: Amsterdam, The Netherlands, 2021; pp. 475–495.

15. Ngayakamo, B.H.; Bello, A.; Onwualu, A.P. Development of eco-friendly fired clay bricks incorporated with granite and eggshell wastes. *Environ. Chall.* **2020**, *1*, 100006. [[CrossRef](#)]
16. Adegoke, D.; Afuwape, R.; Olukanni, D.; Bamigboye, G. Utilization of Palm Fruit Fibers as Constituent Materials for Hand Mould Clay Bricks. *J. Physics Conf. Ser.* **2019**, *1378*, 022044. [[CrossRef](#)]
17. Joglekar, S.N.; Kharkar, R.A.; Mandavgane, S.; Kulkarni, B.D. Sustainability assessment of brick work for low-cost housing: A comparison between waste based bricks and burnt clay bricks. *Sustain. Cities Soc.* **2018**, *37*, 396–406. [[CrossRef](#)]
18. Kazmi, S.M.; Abbas, S.; Saleem, M.A.; Munir, M.J.; Khitab, A. Manufacturing of sustainable clay bricks: Utilization of waste sugarcane bagasse and rice husk ashes. *Constr. Build. Mater.* **2016**, *120*, 29–41. [[CrossRef](#)]
19. Stanislas, T.T.; Komadja, G.C.; Ngasoh, O.F.; Obianyo, I.I.; Tendo, J.F.; Onwualu, P.A.; Junior, H.S. Performance and Durability of Cellulose Pulp-Reinforced Extruded Earth-based Composites. *Arab. J. Sci. Eng.* **2021**, *46*, 11153–11164. [[CrossRef](#)]
20. Singh, A.K.; Mastro, R.E.; Hazra, B.; Esterle, J.; Singh, P.K. Utilization of Coal and Biomass Ash. In *Ash from Coal and Biomass Combustion*; Springer Science and Business Media LLC: Berlin/Heidelberg, Germany, 2020; pp. 37–89.
21. Lozano-Miralles, J.A.; Hermoso-Orzáez, M.J.; Martínez-García, C.; Rojas-Sola, J.I.J.S. Comparative study on the environmental impact of traditional clay bricks mixed with organic waste using life cycle analysis. *Sustainability* **2018**, *10*, 2917. [[CrossRef](#)]
22. Adetayo, O.A.; Umego, O.M.; Faluyi, F.; Odetoeye, A.O.; Bucknor, A.O.; Busari, A.A.; Sanni, A. Evaluation of Pulverized Cow Bone Ash and Waste Glass Powder on the Geotechnical Properties of Tropical Laterite. *Silicon* **2021**, 1–10. [[CrossRef](#)]
23. Neuman, W.F.; Neuman, M.W. The Nature of the Mineral Phase of Bone. *Chem. Rev.* **1953**, *53*, 1–45. [[CrossRef](#)]
24. Bih, N.L.; Mahamat, A.A.; Hounkpè, J.B.; Onwualu, P.A.; Boakye, E. The Effect of Polymer Waste Addition on the Compressive Strength and Water Absorption of Geopolymer Ceramics. *Appl. Sci.* **2021**, *11*, 3540. [[CrossRef](#)]
25. Pavlova, I.A.; Getman, A.A.; Farafontova, E.P. The Possibility of Using Tyumen Keramzite Clay in the Production of Ceramic Materials. *IOP Conf. Series Mater. Sci. Eng.* **2020**, *969*, 012030. [[CrossRef](#)]
26. Luo, H.; Li, Y.B.; Li, S.J.; Chen, R.Y.; Xiang, R.F.; Na Xu, N.; Wang, Q.H.; Si, O.Y. Fabrication of Porous Mullite Ceramics with Different Phase of Alumina for Insulation Materials. *Solid State Phenom.* **2018**, *281*, 242–248. [[CrossRef](#)]
27. Johari, I.; Said, S.; Hisham, B.; Bakar, A.; Ahmad, Z.A. Effect of the change of firing temperature on microstructure and physical properties of clay bricks from Beruas (Malaysia). *Sci. Sinter.* **2010**, *42*, 245–254. [[CrossRef](#)]
28. Heniegal, A.M.; Ramadan, M.A.; Naguib, A.; Agwa, I.S. Case Studies in Construction Materials. *Case Stud. Constr. Mater.* **2020**, *13*, e00397.
29. Monteiro, S.; Vieira, C. Solid state sintering of red ceramics at lower temperatures. *Ceram. Int.* **2004**, *30*, 381–387. [[CrossRef](#)]
30. Herek, L.C.; Hori, C.E.; Reis, M.H.M.; Mora, N.D.; Tavares, C.R.G.; Bergamasco, R. Characterization of ceramic bricks incorporated with textile laundry sludge. *Ceram. Int.* **2012**, *38*, 951–959. [[CrossRef](#)]
31. Pérez-Villarejo, L.; Eliche-Quesada, D.; Iglesias-Godino, F.J.; Martínez-García, C.; Corpas-Iglesias, F.A. Recycling of ash from biomass incinerator in clay matrix to produce ceramic bricks. *J. Environ. Manag.* **2012**, *95*, S349–S354. [[CrossRef](#)]
32. Obianyo, I.; Onwualu, A.P.; Soboyejo, A.B. Mechanical behaviour of lateritic soil stabilized with bone ash and hydrated lime for sustainable building applications. *Case Stud. Constr. Mater.* **2020**, *12*, e00331. [[CrossRef](#)]
33. Bhuiya, A.W.; Hu, M.; Sankar, K.; Keane, P.F.; Ribero, D.; Kriven, W.M. Bone ash reinforced geopolymer composites. *J. Am. Ceram. Soc.* **2021**, *104*, 2767–2779. [[CrossRef](#)]
34. British Standards Institution. *British Standard Specification for Clay Bricks*; British Standards Institution: London, UK, 1985.
35. Zhao, X.; Liu, Q.; Yang, J.; Zhang, W.; Wang, Y. Sintering Behavior and Mechanical Properties of Mullite Fibers/Hydroxyapatite Ceramic. *Materials* **2018**, *11*, 1859. [[CrossRef](#)] [[PubMed](#)]
36. Miron, G.D.; Kulik, D.A.; Yan, Y.; Tits, J.; Lothenbach, B. Extensions of CASH+ thermodynamic solid solution model for the uptake of alkali metals and alkaline earth metals in C-S-H. *Cem. Concr. Res.* **2021**, *152*, 106667. [[CrossRef](#)]
37. Mendoza-Castillo, D.I.; Bonilla-Petriciolet, A.; Jáuregui-Rincón, J.J.D.; Treatment, W. On the importance of surface chemistry and composition of bone char for the sorption of heavy metals from aqueous solution. *Porous Mater. Theory Its Appl. Environ. Remediat.* **2015**, *54*, 1651–1662. [[CrossRef](#)]
38. Rezaee, A.; Ghanizadeh, G.; Behzadiyannejad, G.; Yazdanbakhsh, A.; Siyadat, S.D. Adsorption of Endotoxin from Aqueous Solution Using Bone Char. *Bull. Environ. Contam. Toxicol.* **2009**, *82*, 732–737. [[CrossRef](#)] [[PubMed](#)]
39. Malla, K.P.; Regmi, S.; Nepal, A.; Bhattarai, S.; Yadav, R.J.; Sakurai, S.; Adhikari, R. Extraction and Characterization of Novel Natural Hydroxyapatite Bioceramic by Thermal Decomposition of Waste Ostrich Bone. *Int. J. Biomater.* **2020**, *2020*, 1–10. [[CrossRef](#)] [[PubMed](#)]
40. Chakraborty, R.; Das, S.; Bhattacharjee, S.K. Optimization of biodiesel production from Indian mustard oil by biological tri-calcium phosphate catalyst derived from turkey bone ash. *Clean Technol. Environ. Policy* **2014**, *17*, 455–463. [[CrossRef](#)]
41. Rana, M.; Akhtar, N.; Rahman, S.; Jamil, H.M.; Asaduzzaman, S.M. Extraction of hydroxyapatite from bovine and human cortical bone by thermal decomposition and effect of gamma radiation: A comparative study. *Int. J. Complementary Altern. Med.* **2017**, *8*, 1–10.
42. Sun, Z.; Cui, H.; An, H.; Tao, D.; Xu, Y.; Zhai, J.; Li, Q. Synthesis and thermal behavior of geopolymer-type material from waste ceramic. *Constr. Build. Mater.* **2013**, *49*, 281–287. [[CrossRef](#)]
43. Younesi, M.; Javadpour, S.; Bahrololoom, M.E. Effect of Heat Treatment Temperature on Chemical Compositions of Extracted Hydroxyapatite from Bovine Bone Ash. *J. Mater. Eng. Perform.* **2011**, *20*, 1484–1490. [[CrossRef](#)]
44. Ifka, T.O.; Palou, M.T.; Bazelova, Z. Influence of CaO and P₂O₅ of bone ash upon the reactivity and the burnability of cement raw mixtures. *Ceram. Silikáty* **2012**, *56*, 76–84.

45. British Standards Institution. *Methods of Test for Soils for Civil Engineering Purposes: Classification Tests*; British Standards Institution: London, UK, 1990.
46. Bennour, A.; Mahmoudi, S.; Srasra, E.; Boussen, S.; Htira, N. Composition, firing behavior and ceramic properties of the Sejnène clays (Northwest Tunisia). *Appl. Clay Sci.* **2015**, *115*, 30–38. [[CrossRef](#)]
47. Eliche-Quesada, D.; Sandalio-Pérez, J.A.; Martínez-Martínez, S.; Pérez-Villarejo, L.; Sánchez-Soto, P.J. Investigation of use of coal fly ash in eco-friendly construction materials: Fired clay bricks and silica-calcareous non fired bricks. *Ceram. Int.* **2018**, *44*, 4400–4412. [[CrossRef](#)]
48. Achik, M.; Benmoussa, H.; Oulmekki, A.; Ijjaali, M.; El Moudden, N.; Touache, A.; Álvaro, G.G.; Rivera, F.G.; Infantes-Molina, A.; Eliche-Quesada, D.; et al. Evaluation of technological properties of fired clay bricks containing pyrrhotite ash. *Constr. Build. Mater.* **2021**, *269*, 121312. [[CrossRef](#)]
49. Standard, ASTM. *Standard Test Methods for Sampling and Testing Brick and Structural Clay Tile*; ASTM: West Conshohocken, PA, USA, 2014; p. C67-14.